tvst

https://doi.org/10.1167/tvst.7.6.19

Article

Fluidics of Single and Double Blade Guillotine Vitrectomy Probes in Balanced Salt Solution and Artificial Vitreous

Mario Rosario Romano[1], Alessandro Stocchino[2], Mariantonia Ferrara[1], Alberto Lagazzo[2], and Rodolfo Repetto[2]

[1] Department of Biomedical Sciences, Humanitas University, Rozzano - Milano, Italy
[2] Department of Civil, Chemical and Environmental Engineering, University of Genoa DICCA, Genoa, Italy

Correspondence: Alessandro Stocchino, Department of Civil, Chemical and Environmental Engineering, University of Genoa, Via Montallegro 1, 16145, Genoa, Italy. e-mail: alessandro.stocchino@unige.it

Received: 16 May 2018
Accepted: 27 September 2018
Published: 6 December 2018

Keywords: fluidics of vitrectomy; Particle Image Velocimetry; flow rate measurements

Citation: Romano MR, Stocchino A, Ferrara M, Lagazzo A, Repetto R. Fluidics of single and double blade guillotine vitrectomy probes in balanced salt solution and artificial vitreous. Trans Vis Sci Tech. 2018; 7(6):19, https://doi.org/10.1167/tvst.7.6.19

Purpose: To assess the fluidics of double-vitreous cutter blade (DB) compared with single-blade (SB) guillotine with 23-, 25-, and 27-gauge vitrectomy probes. To assess flow characteristics and flow rates in viscous and viscoelastic fluids.

Methods: We used Particle Image Velocimetry to measure the flow field close to the tip of each cutter probe and we derived kinematic quantities of interest, such as kinetic energy and acceleration. We performed measurements both on a balanced salt solution (BSS) and on a viscoelastic artificial vitreous (AV).

Results: The flow rate is significantly higher with DB than SB vitrectomy probes, for a given pumping pressure and cutting rate. The fluid flow observed is very different between BSS and AV tests.

Conclusions: The DB has more efficient fluidics than SB vitrectomy probe in all tested conditions. Fluid acceleration depends on the cutting frequency, especially in the case of measurements in AV. The flow rate strongly depends on the pressure and it is little affected by the cutting frequency, in a range of clinical interest. The 27-G DB produces flow rates similar to the 23- and 25-G SB, with significantly smaller acceleration. The flow induced in the AV is different from that in BSS and oscillates at different frequencies.

Translational Relevance: DB cutters prove to be more efficient in terms of lower acceleration for a given flow rate. The latter is mainly controlled by aspiration pressure and less by cut rates. The influence of vitreous rheology deserves further investigations.

Introduction

In the last decades pars plana vitrectomy (PPV) has been characterized by dramatic changes in terms of smaller and faster systems.[1] The main issue associated with the vitrectomy procedure is the generation of vitreoretinal tractions by the vitreous cutter, with consequent iatrogenic retinal breaks and inadvertent removal of unwanted tissue, especially in the presence of detached retina.

Flow rate and fluid acceleration have been shown to be significantly related to retinal tractions and efficiency in vitreous removal.[2] In particular, fluid acceleration represents a fundamental kinematic quantity, because it is closely related to pressure variations in the vitreous and, consequently, stresses on the retina. Therefore, for a safe and efficient vitrectomy, optimization of fluidics can be achieved by maximizing the flow rate and minimizing the acceleration around the cutter port.

To control the flow rate, vitrectomy machines are equipped with peristaltic (flow control) or venturi (vacuum control), or a combined peristaltic/venturi pumps. Recently, a new fluidics control system, called VacuFlow Valve Timing intelligence (VTi), has been developed to provide both instantaneous vacuum and flow mode aspiration, enhancing intraoperative fluidics stability, and potentially reducing flow fluctuations.[3]

Vitreous cutters can be classified on the basis of the cutting edges: single-blade (SB) guillotine (regular

blade) and double-cutting blades (DB), both currently available in different sizes and port geometrical design. DB cutters have been found to have several advantages over SB ones. Previous studies have highlighted that DB cutters, owing to their better duty cycle, are capable of producing larger flow rates, which allows the user to overcome the limits of smaller needles, related to the reduced flow rate and vitreous chamber stability.[3,4] In 23-, 25-, and 27-G SB probes it has been demonstrated that, for a fixed aspiration pressure, a biased open-duty cycle is associated with a decrease in flow rate as the cut rate increases and the opposite happens for the biased closed-duty cycle. In the case of the 50/50 duty cycle the flow rate was found to only slightly increase with the cut rate.[5] In DB cutters the duty cycle is optimized to virtually 100% because the port is never completely closed, allowing smoother flow with continuous cutting, regardless of blade position and cut speed.[3,4,6] DB probes cut vitreous twice during each cycle due to the presence of two cutting edges, which effectively doubles the cut rate up to 16,000 cpm. Moreover, the vitreous is also kept engaged to the DB port during the entire cycle movement, without abrupt vitreous incarcerations.[4]

It has been postulated that, being the vitreous a viscoelastic and heterogeneous fluid, higher cut-rates fragment the vitreous into smaller pieces, resulting in reduced vitreal viscosity and resistance to flow.[7] The hypothesis of reduced vitreous viscosity related to the generation of smaller vitreous fragments was not supported by recent data, which showed that the hydraulic resistance did not change using SB and DB cutters at cutting rates over 1500 and 2000 cpm, respectively.[8] It has also been shown experimentally that increasing the cutting frequency reduces retinal tractions.[9]

Teixerira et al.[10,11] developed a method to quantify the retinal traction exerted by vitreous cutters, identifying several significant factors, such as cut speed, vacuum rate, cutter size, and distance between cutter and retina. The authors found that retinal tractions decreased at higher cut rates and increased with higher aspiration vacuum and greater closeness to the retina. Moreover, cutter size appeared to be directly related to the strength of traction,[2] as recently confirmed by the demonstration of the progressive shortening of membrane attraction distance decreasing the cutter gauge.[4] However, using smaller gauge instrumentation and high cut rates, a high aspiration pressure is required to achieve effective vitreous removal and reasonable flow rates.[12]

Several experimental works on vitrectomy fluidics have been carried out using BSS solutions or egg albumen.[13–17] Experiments on vitreous from animal eyes have also been performed.[5,15,18] The above studies focused on the measurement of the flow rate and its dependency on the working conditions. In recent years Particle Image Velocimetry (PIV) measurements have been introduced to measure the flow field around the tip of vitreous cutters in vitro.[2] The use of this optical technique increases significantly the amount of information that can be obtained from experiments, because the spatial and temporal evolution of the velocity field can be measured on different planes, which allows one to compute various kinematic quantities, such as fluid acceleration and kinetic energy.

In this study we performed PIV measurements of the fluidic of DB and SB guillotine with 23-, 25-, and 27-G vitrectomy probes, under various surgical scenarios. Measurements have been taken both in BSS and using an artificial viscoelastic vitreous, of which we measured the rheologic properties, showing that they are similar to those of the real vitreous. Using an artificial vitreous instead of egg albumen or pig eyes allows for a reliable experiment reproducibility.

Material and Methods

Experimental Setup

We studied the flow induced by different cutters connected to the EVA vitrectomy system (DORC International, Zuidland, The Netherlands), equipped with the VTi control system. We performed experiments with different cutters (23, 25, and 27 G) and, for each gauge, we tested both the high speed SB and DB (named two-dimensional cutter, TDC) in a cubical experimental chamber (dimension $3 \times 3 \times 3$ cm), filled with either balanced salt solution (BSS) or an artificial vitreous (AV). The chamber employed in the present study is similar to the one used in Rossi et al.[2]

Particle Image Velocimetry and Postprocessing of the Experimental Data

The flow field induced by the vitreous cutter was measured using PIV, which is an optical technique used to measure the motion of fluids.[19] In the standard configuration, measurements are taken on

a plane on which it is assumed that the flow is almost two-dimensional (or axisymmetric).

For the present experiments, we used a solid-state laser (wave length of 532 nm, continuous emission with variable power, up to 2 W; Laser Quantum Ltd, Stockport, UK), a high-speed digital camera (model IDT Xstream Xs3; Integrated Design Tools, Pasadena, CA), with a resolution of 1280×1024 pixels and a maximum acquisition frequency of 25,000 fps depending on the selected resolution. We mounted a 90-mm macro lens (Tamron SP AF 90-mm F/2.8; Tamron Europe GmbH, Cologne, Germany) on the camera, in order to obtain a field of view around the cutter aperture ranging from 14×18 mm to 9×11 mm, depending on the selected resolution. With the chosen PIV settings, we measured from a minimum of 7 to a maximum of 25 velocity fields with a cutting cycle, depending on the cutting rate.

From the measured velocity fields $\boldsymbol{u}(x, y, t)$, we derived various quantities of interest; in particular, we computed fluid acceleration $\boldsymbol{a}$, defined as:

$$\boldsymbol{a} = \frac{\partial \boldsymbol{u}}{\partial t} + (\boldsymbol{u} \cdot \nabla)\boldsymbol{u}. \quad (1)$$

Note that the acceleration consists of the sum of the local time derivative of the velocity and the convective acceleration, which accounts for spatial derivatives of $\boldsymbol{u}$. We also computed the fluid kinetic energy per unit mass k, defined as $k = \frac{1}{2}\boldsymbol{u} \cdot \boldsymbol{u}$.

In the present study, we make extensive use of quantities obtained through spatial and temporal averages of the local and instantaneous measured quantities. Spatial averaged quantities have been calculated over a circular area centered in correspondence of the cutter port and with a radius of 3 mm. Obviously, the values of spatially averaged quantities depend on the size of the region over which the spatial average is taken.

Flow Rate Measurements

In order to measure the flow rate for a set of operational parameters, we took pictures of a vertical plane of the whole reservoir containing the fluid. Tracking in time the position of the interface from the images, surface position accuracy of ≈14 μm, and knowing the cross-sectional area of the reservoir, we evaluated the flow rate pumped by the vitreous cutter with an accuracy of ≈0.68 mL/min. With this method we were able to measure the "average" flow rate, disregarding the small oscillations occurring during a cutting cycle.

Working Fluids

We performed two series of experiments using different fluids. In the first series, the vitreous cutter was tested in a BSS, which is representative, from the mechanical point of view, of an extensively liquefied vitreous and is a Newtonian fluid.

In the second series of experiments, we adopted a vitreous phantom, referred to as AV in the following, with properties similar to those of the real healthy vitreous. This was prepared as a solution of acid sodium salt (HA) mixed in deionised water, without adding the agar powder as proposed in Kummer et al.,[20] with the aim to produce a perfectly transparent fluid that is a strict requirement for PIV.

In order to guarantee the reproducibility of measurements and to characterize the mechanical properties of the AV we performed rheologic test. In particular, we carried out oscillatory tests by subjecting the material sample to harmonic periodic strains γ of small amplitude and measuring the corresponding stress τ. The output of the tests are two moduli, called the elastic G' and loss G'' moduli, see Tanner.[21] The former is a measure of the elasticity of the fluid and the latter of its viscosity. We also performed steady rheologic tests, studying the stress generated in the fluid when the sample was subjected to a constant shear rate $\dot{\gamma}$.

All rheologic tests were performed with the rotational viscometer Physica Anton Paar MCR 301 (Anton Paar Italia s.r.l, Rivoli, Italia). The instrument is equipped with a synchronous motor, with a high-resolution optical encoder and an air bearing, to allow a torque resolution of 0.1 nN·m in a range between 0.05μN·m and 200 mN·m. Measurements were taken both at 23°C and 37°C.

In Figure 1a we show the two moduli G' and G'' of the fluid AV versus the oscillation frequency. We note that our results are quite close to those relative to porcine vitreous. In fact Nickerson et al.[22] found $G' = 10$ Pa and $G'' = 3.9$ Pa at 10 rad/s and Swindle et al.[23] found $G' = 3.46$ Pa and $G'' = 0.71$ Pa at 12.57 rad/s. Moreover, both Nickerson et al.[22] and Sharif-Kashani et al.[24] found on porcine vitreous that G' and G'' grow with the testing frequency, as we also observe in our rheologic tests.

The results of the tests performed at a constant rotational velocity are reported in Figure 1b right panel. It appears that the fluid has shear thinning properties, because the slope of the stress rate of strain curve decreases with $\dot{\gamma}$. This means that the apparent viscosity decreases as the shear rate grows.

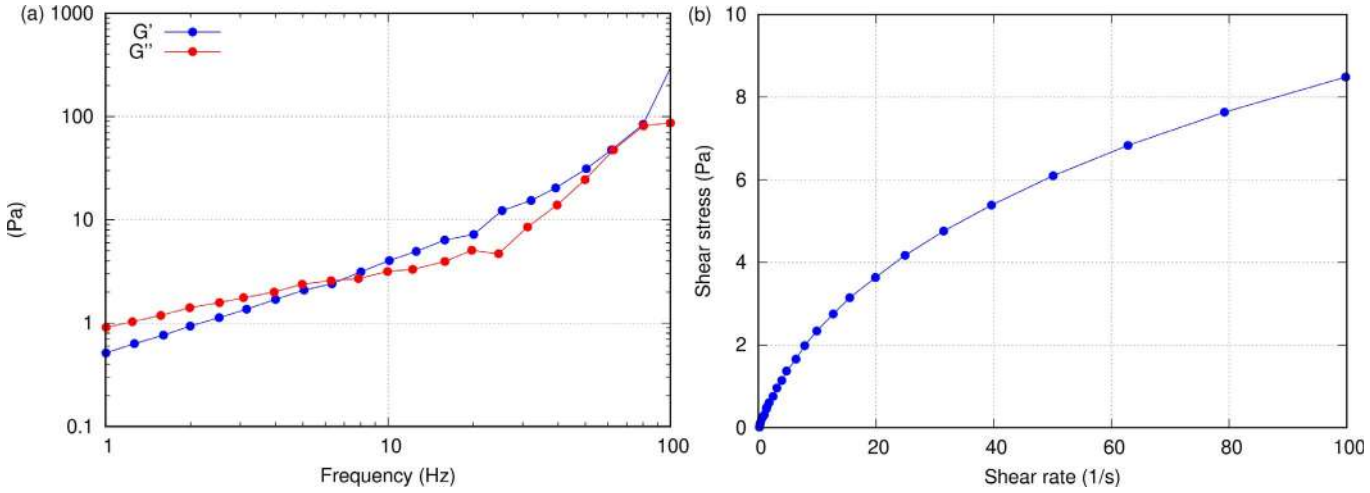

Figure 1. (a) Storage G' and loss G'' moduli versus the oscillation frequency f (1–100 Hz). Strain $\gamma = 0.05$. (b) Shear stress τ versus shear rate γ. Temperature, T = 23°C. Note that the dependency of the complex modulus on the strain is relatively small, lower than 10%. Measurements at 37°C are not shown, owing to the relatively small dependence of the moduli on temperature, of the order of 40% for G' and less than 20% for G''.

Description of the Experiments

We performed experiments with three different cutters (23, 25, and 27 G). For each gauge we tested both SB and TDC cutters. Moreover, for each case we considered "core" and "shaving" working modalities of the device. For all configurations we took measurements on two different planes, one across the cutter gap ("lateral view") and one orthogonal to it ("frontal view"). In the following sections, the plane of measurement and the position of the port will be indicated in the figures. With BSS we performed two series of experiments. In the first (BSS1), we used the cutters with settings typical in the surgical practice (in terms of pumping pressure/flow rate and cutting frequency). In the second series (BSS2), we fixed either the pressure or the cutting frequency and varied the other, in order to understand the role of each parameter on the performance of the cutter. With AV we only performed experiments in "core vitrectomy" mode in similarity with experiments of BSS2. In the Table we report a summary of all experiments performed.

Results

Experiments With BSS

Figure 2 shows the results of a typical experiment with BSS, showing maps of the time averaged velocity (Fig. 2a) and acceleration (Fig. 2b) magnitudes on a frontal plane of measurement, with the cutter port facing the reader. We note that the quality of the measured flow fields was comparable in all experiments and, therefore, the choice of this specific experiment shown in the figure is arbitrary. In both maps of Figure 2 we show the flow on the front view. The velocity field, Figure 2a, is very regular and the slight departure from symmetry could be attributed to vibrations of the cutter and experimental error. The velocity field on the lateral view looks very similar (not shown); therefore, we can conclude that in the case of BSS the flow approximately satisfies a radial symmetry and resembles the flow induced by a point sink.

One of the main observables of the present analysis is fluid acceleration,[25] the time average of which is shown in Figure 2b. From our measurements we could compute both terms of Equation 1 and we found that the convective term is largely subdominant assuming, in all cases, values approximately 1 to 4 mm/s^2, whereas the time derivative of the velocity is always of the order of 10^2 mm/s^2.

The power spectra of the kinetic energy per unit mass show that, in all cases, a clear peak in the power spectrum is present in correspondence of the cutting frequency (i.e., 100 Hz corresponding to 6000 cpm, see Fig. 3). This is a good indication of the fact that the experiments properly resolved this time scale. Peaks corresponding to the superharmonics of the cutting frequency were also found, because the cutter motion was not monochromatic.

Regarding the experiments of the series BSS2, the flow rate is reported as a function of the cutting

Table. Table of the Parameters Characterizing the Experiments

Working Fluid	Cutter	Mode	Pressure, mm Hg	cpm	Flow, mL/min	*N* Runs
Experiment series BSS1: clinical parameters						
BSS	23 SB	Core vitrectomy	400	5000	-	1
	23 SB	Shaving	200	8000	4	1
	23 TDC	Core vitrectomy	400	5000	-	1
	23 TDC	Shaving	200	8000	4	1
	25 SB	Core vitrectomy	600	6000	-	1
	25 SB	Shaving	200	8000	4	1
	25 TDC	Core vitrectomy	600	6000	-	1
	25 TDC	Shaving	200	8000	4	1
	27 TDC	Core vitrectomy	600	6000	-	1
	27 TDC	Shaving	200	8000	4	1
Experiment series BSS2: pressure and cpm dependence						
BSS	23 SB	Core vitrectomy	300–600	5000–8000	-	8
	23 TDC	Core vitrectomy	300–600	5000–8000	-	8
	25 SB	Core vitrectomy	300–600	5000–8000	-	8
	25 TDC	Core vitrectomy	300–600	5000–8000	-	8
	27 TDC	Core vitrectomy	300–600	5000–8000	-	8
Experiment series AV: pressure and cpm dependence						
AV	23 SB	Core vitrectomy	300–600	1000–8000	-	11
	23 TDC	Core vitrectomy	300–600	1000–8000	-	11
	25 SB	Core vitrectomy	300–600	1000–8000	-	11
	25 TDC	Core vitrectomy	300–600	1000–8000	-	11
	27 SB	Core vitrectomy	300–600	5000–8000	-	8
	27 TDC	Core vitrectomy	300–600	1000–8000	-	11

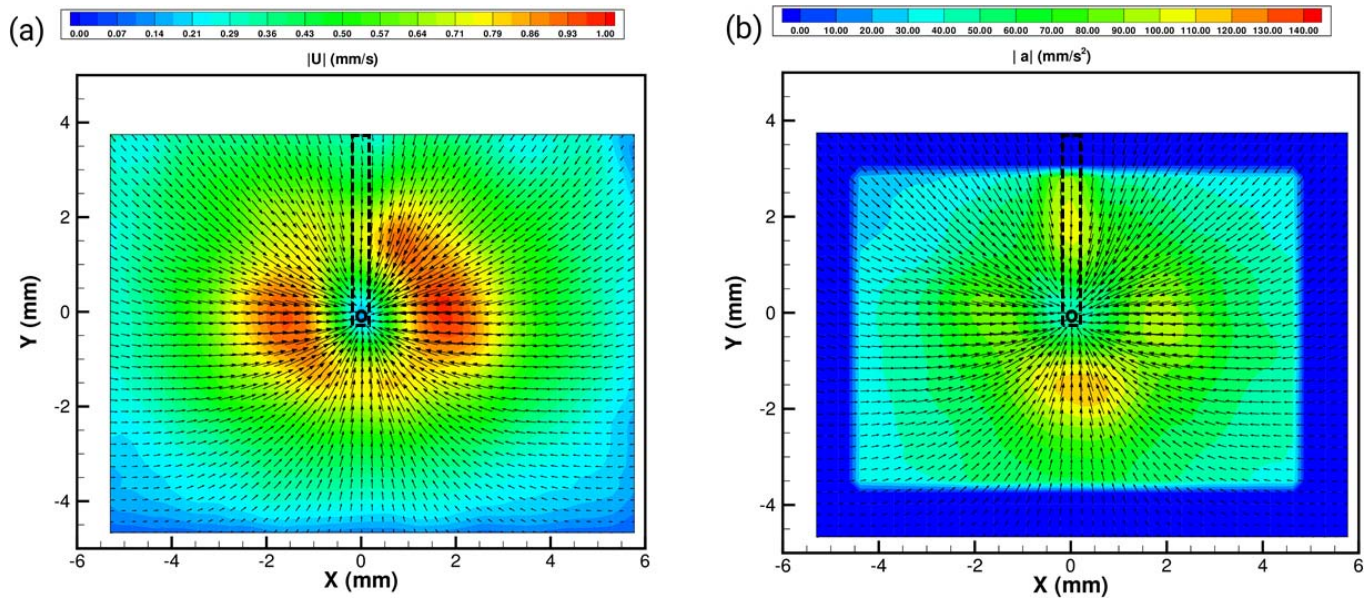

Figure 2. Time-averaged maps of the magnitude of (a) velocity and (b) acceleration. In both panels *arrows* represent time averaged velocity vectors. The position of the cutter is indicated in the figure and the cutter port (*black hollow circle*) is centered in $x = (0, 0)$. Experiment with BSS, 25-G cutter, SB, and core mode. Note that we did not compute the acceleration close to the image border, because we used a least square centered scheme for spatial derivatives, which requires five measurement points, not available close to the boundary of the domain.

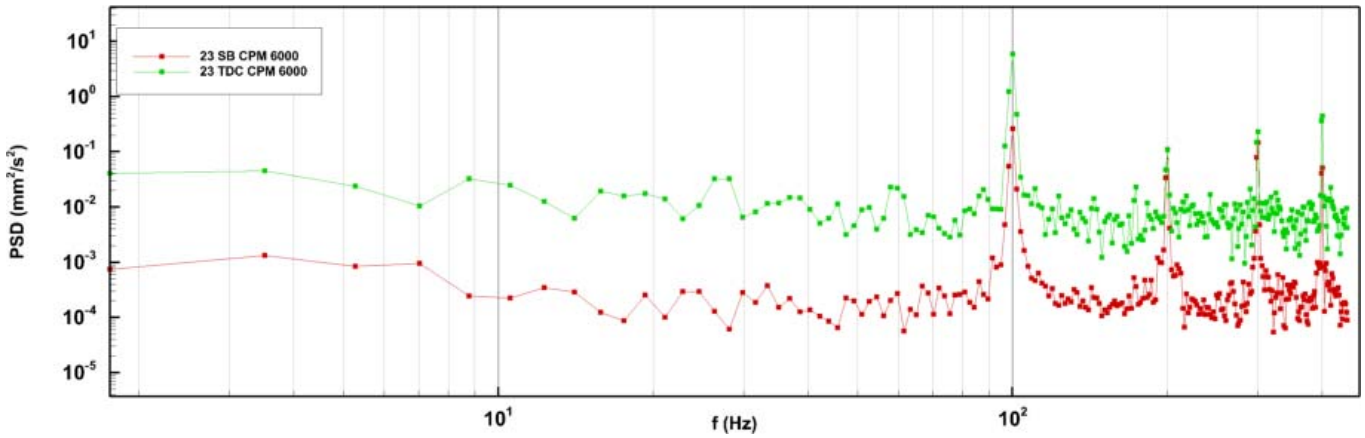

Figure 3. Power spectra of the fluid kinetic energy per unit mass. Experiments with BSS, pressure = 600 mm Hg, cpm 6000.

frequency for all vitreous cutters in core mode in Figure 4a. The flow rate has a very weak dependency of the cutting frequency. Moreover, for a given cutting frequency, the dependency of flow rate on the pressure was found to be linear to a very good degree of approximation in all cases (Fig. 4b).

Figure 4c shows how time and space averaged fluid acceleration depends on the cutting frequency. The

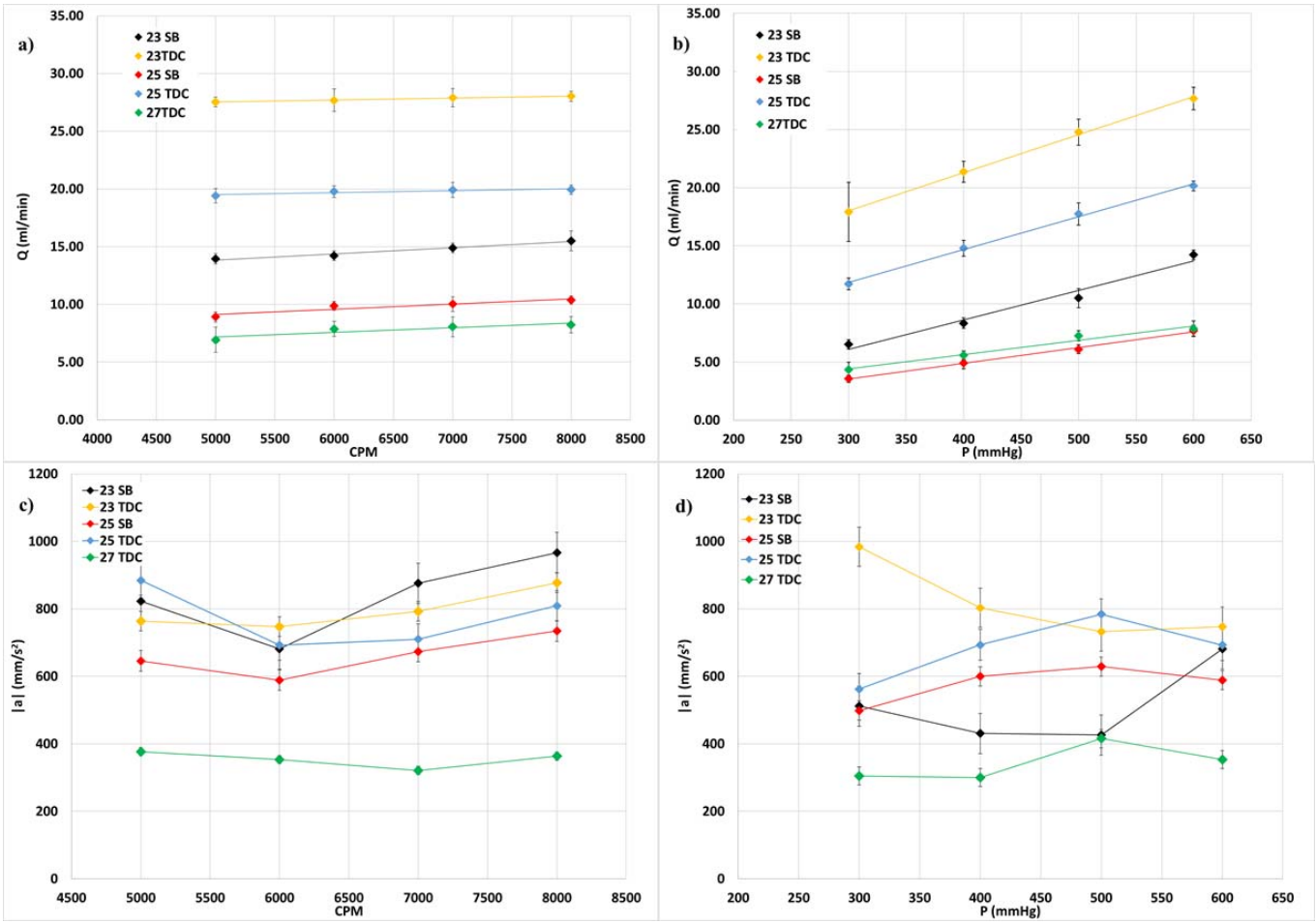

Figure 4. Flow rate versus the cutting frequency (a) and the sucking pressure (b). Space and time averaged acceleration versus the cutting frequency (c) and the sucking pressure (d). Experiments in BSS. Pressure = 600 mm Hg .

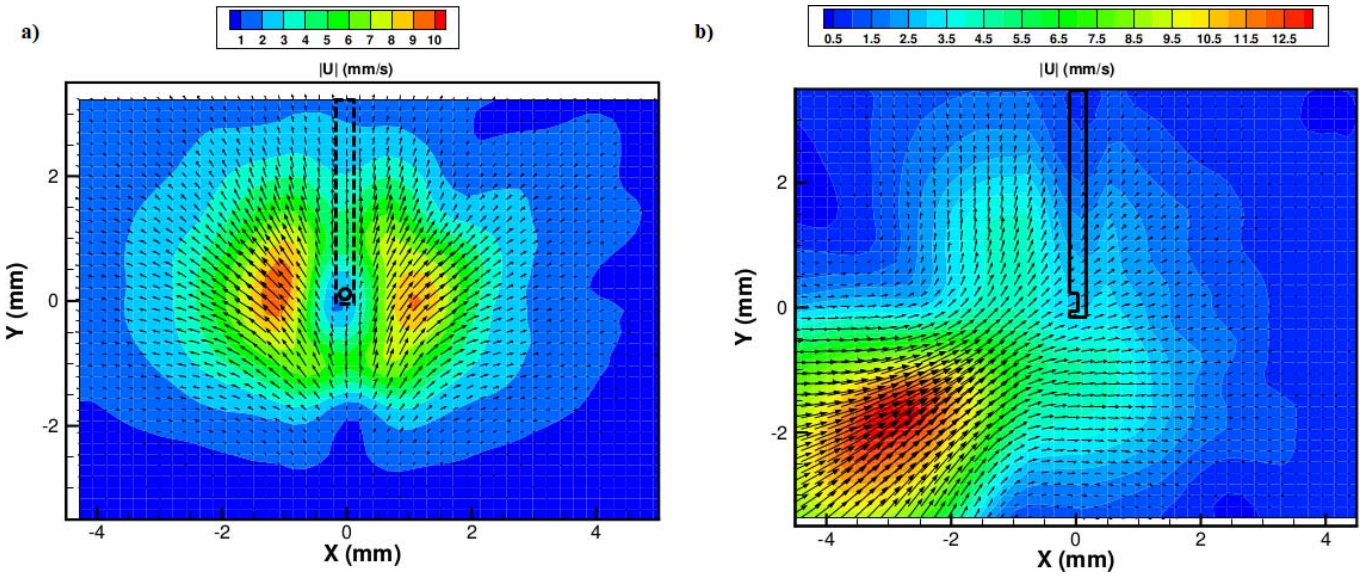

Figure 5. Time-averaged maps of velocity magnitude and velocity vectors. The needle is located along the axis $x = 0$ (for $y > 0$) and the port is centered in the point $x = (0, 0)$, the position of the cutter is sketched on each map. (a) Front view, (b) lateral view with the cutter port on the negative side of the x-axis. Twenty-five gauge, TDC, core mode, and 4000 cpm.

results do not show a clear trend, but in all cases a minimum acceleration exists, for a cutting frequency of approximately 6000 cpm (7000 for the case of SB 25-G cutter). The magnitude of the acceleration induced by the SB and the TDC cutters is similar in spite of the fact the TDC is capable of pumping more than twice as much fluid than the SB.

Finally, Figure 4d shows the dependency of the average acceleration on the pressure. The results do not show a clear trend.

Experiments With AV

In Figure 5, we report time averaged maps of the velocity field on the "front" and "lateral" views. The flow field is remarkably different in this case with respect to experiments with the BSS solution (see Fig. 2a for a comparison). In the case of BSS the flow has approximately a radial symmetry and, interestingly enough, such a symmetry is lost in the case of a viscoelastic fluid. Figure 5b shows that the flow remains confined within a relatively narrow region facing the cutter port and inclined with respect to the needle by an angle greater than right. Out of this confinement region of the flow the velocity is directed away from the cutter (Fig. 5). The complete details of the flow are difficult to grasp from knowledge of the velocity field only on two orthogonal planes; the experiments suggest, however, the existence of a complicated and highly three-dimensional flow field, whereby fluid particles move away from the needle port everywhere but in a relatively narrow region of flow confinement in front of the needle aperture. In this confinement region, the velocity attains large values and also decays quite slowly with the distance from the needle. Qualitatively similar results were obtained for all cutters and all operating conditions.

A notable difference between SB and TDC, however, is the orientation of the confinement region with respect to the cutter needle. In the SB case, at low values of the cutting frequency the confinement region (and thus the main flow direction) is approximately at a right angle with the needle. This angle decreases at higher cutting frequencies and becomes acute, whereas the angle is always obtuse in the case of the TDC cutter and decreases with the cutting frequency.

In Figure 6, we report power spectra of the kinetic energy of the flow, analogous to those of Figure 3. The power spectra obtained with the experiments with AV have common features that distinguish them from those relative to BSS tests. The spectra shown in the figure have many clear peaks, the most intense of which typically corresponds to the cutting frequency, as in BSS experiments. However, subharmonic and superharmonic frequencies (i.e., submultiples and multiples of the dominant frequency) are typically characterized by higher peaks in the experiments with AV than with BSS. Moreover, the new feature that characterizes the experiments in AV is the existence of a peak (often of significant magnitude) at a frequency

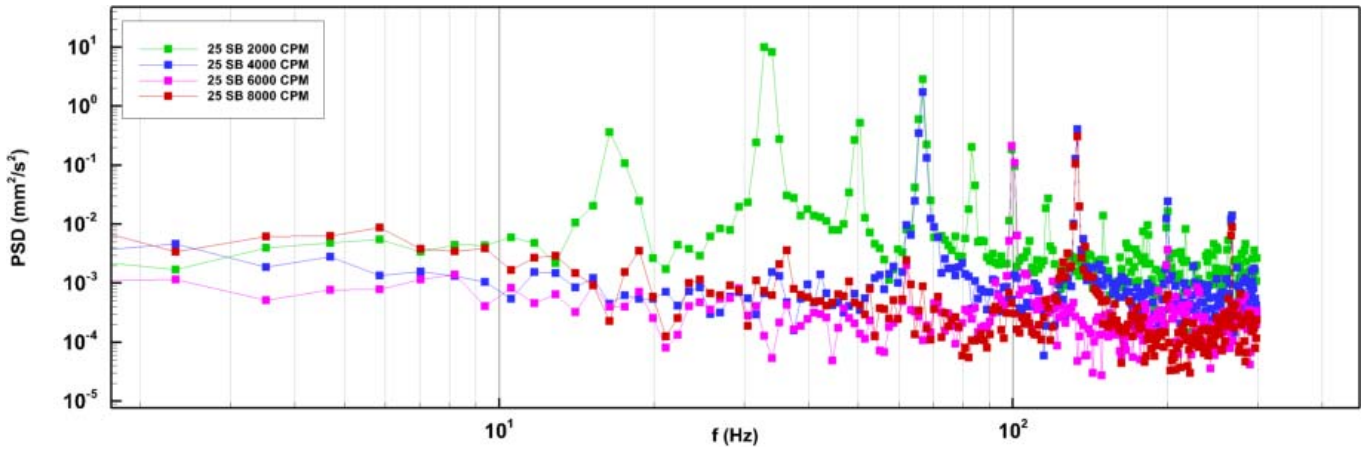

Figure 6. Power spectra of the kinetic energy per unit mass. Each curve corresponds to a different cutter. SB front view. Pressure = 600 mm Hg.

that is not related to the cutting frequency (e.g., the third peak in Fig. 6, green curve). This originates as a consequence of the existence of natural frequencies of oscillation of the system, which is something inherently associated with the elastic component of the fluid. In some cases, such peaks are the most intense.

In Figures 7a to 7d we report plots analogous to those of Figures 4a to 4d for the AV. As for the case of experiments with BSS, we find that the flow rate does not depend strongly on the cutting frequency, Figure 7a. The flow rates are higher for larger cutters and, for a given size, in the case of the TDC cutter. In analogy with the experiments with BSS also in the case of AV the flow rate grows almost linearly with the pressure, the rate of growth being slightly higher for larger needles (Fig. 7b).

In Figure 7c we show how the magnitude of the time and spatially averaged fluid acceleration depends on the cutting frequency. We have adopted the same averaging area in the experiments with AV and BSS, thus the two cases are comparable. The average fluid acceleration decreases with the cutting frequency in all cases but for the 27-G TDC for which it remains approximately constant. This is different with respect to the case of experiments performed with BSS, where the acceleration slightly grew with the frequency (at least for high frequencies). The values of the acceleration obtained with the AV are smaller than those corresponding with BSS.

Finally, Figure 7d shows the dependency of the average fluid acceleration on the pumping pressure. As expected, the acceleration grows with the pressure in all cases. An exception is, again, the 27-G TDC, for which we find that the acceleration is almost independent of the pressure.

Discussion

The aim of this study was to achieve a reliable assessment of fluidics of SB and TDC cutters of different sizes (23, 25, and 27 G), in order to optimize vitrectomy settings. A flow rate as steady as possible is the mainstay for an efficient and safe procedure. Indeed, fluid acceleration has been identified as a crucial causative factor and predictor of retinal traction.[25] We tested all the cutters under several surgical scenarios, setting the parameters in both core and shaving mode as it is commonly done in the surgical practice. We measured the flow field using the PIV technique, which allowed us to obtain a good description of the spatial and temporal evolution of the velocity field near the cutter tip. We adopted both BSS and AV in our experiments, as representative of the liquefied vitreous (BSS) and of the vitreous in its gel phase (AV) in order to reproduce as closely as possible, the working conditions during the vitrectomy. Other authors in the past tested vitreous cutters with non-Newtonian viscoelastic fluids, in particular using egg albumen[2,13–17] or porcine eyes[5,15,18]; however, information on the rheologic properties of the fluids were not provided. Using AV, we could test the rheology of the fluid and tune it in such a way that is has properties similar to those of the healthy vitreous. Moreover, working with a fluid of known composition makes our experiments reproducible.

Interestingly, we found that the flow field in the case of BSS and AV are very different from the qualitative point of view. In the case of experiments with BSS the flow has an almost perfect radial symmetry and resembles the flow induced by a

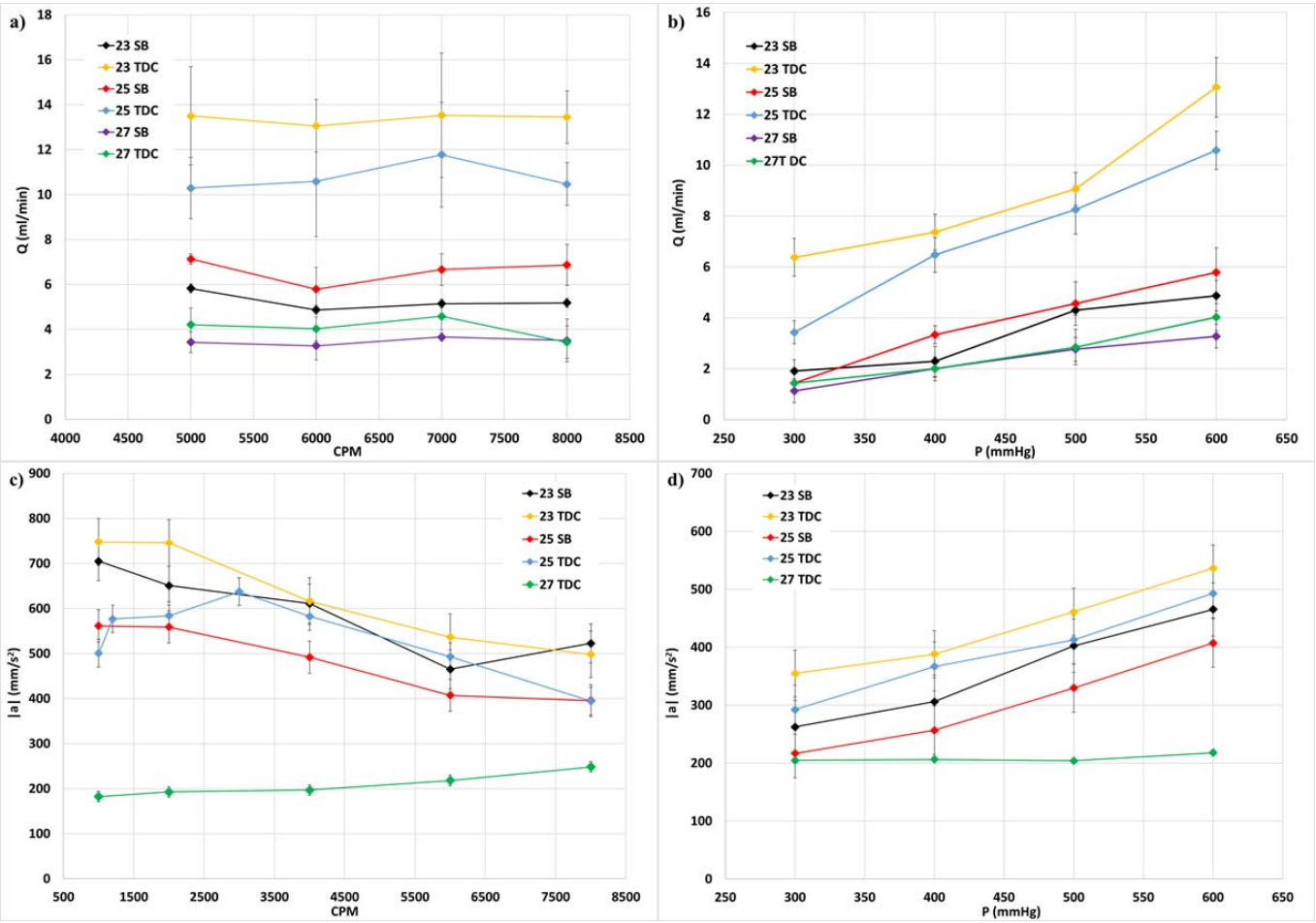

Figure 7. Flow rate versus the cutting frequency (a) and the sucking pressure (b). Space and time averaged acceleration versus the cutting frequency (c) and the sucking pressure (d). Experiments in AV.

three-dimensional sink (see Fig. 2). This symmetry is entirely lost in the case of the viscoelastic vitreous: the motion toward the cutter port keeps confined in a relatively narrow region in front of the port (Fig. 5). This finding is independent of the cutter size and of the device operational conditions and seems in agreement with some of the flow fields shown in Rossi et al.[2,4] This means that different orientations of the cutter during surgery will induce very different mechanical stresses on the retina. Moreover, the velocity decays more slowly moving away from the cutter port in the case of AV than BSS. Thus, in the former case, the region affected by the presence of the cutter is significantly larger. This observation has clinical relevance because it implies that the cutter will transmit stresses to the retina from larger distances if the vitreous is in the gel phase.

Another important difference between the experiments in BSS and AV is related to the fluid response to the unsteady suction generated by the guillotine motion. In the case of BSS, fluid velocity oscillates at the frequency of the cutter and at frequencies that are multiples or submultiples of it. In the case of the AV, on the other hand, we also invariably found an additional frequency in the flow, unrelated to the cutting frequency. This can be interpreted as a "natural frequency" of the system, which arises owing to the elasticity of the fluid and depends on the properties of the fluid and the shape of the domain but not on the motion of the cutter blade. It is known that when a natural frequency of a system exists, it can possibly be resonantly excited by a forcing at a similar frequency. Resonance excitation in a fluid leads to large velocities and accelerations. A similar mechanism is discussed in detail in previous works[26,27] where resonant excitation of vitreous motion induced by eye rotations is studied. Therefore, we conclude that care needs to be taken to avoid

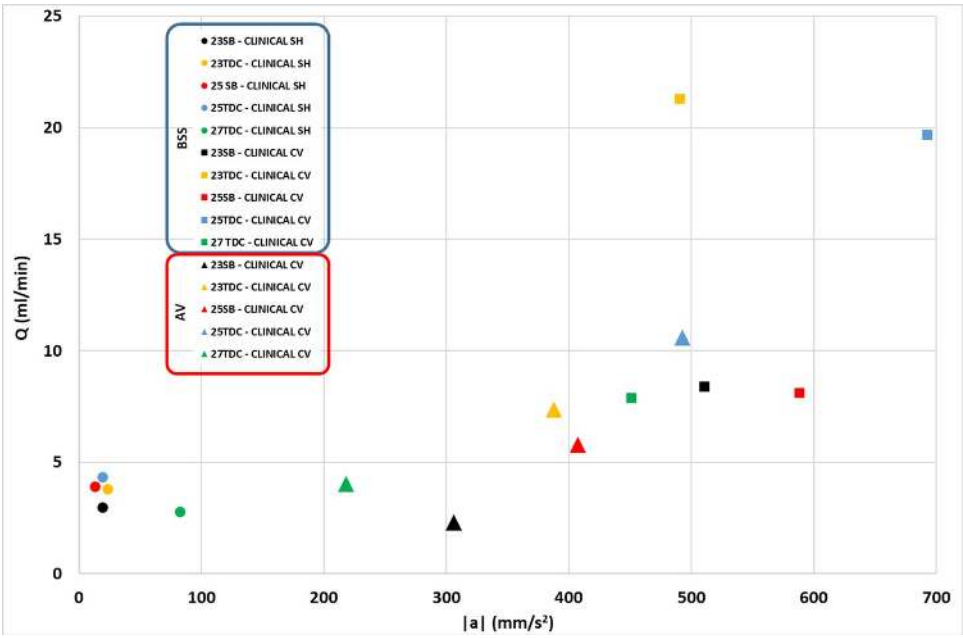

Figure 8. Plot of the flow rate, *Q*, versus the averaged acceleration $|a|$ for all tested cutters in BSS and AV. The experiments plotted refer to common clinical settings for each cutter dimension.

operating the cutter at a frequency close to one of its natural frequencies. We believe that this topic is worth a specific investigation; in particular, it would be interesting to study how variations in fluid properties would affect the system dynamics, an endeavor that is beyond the scope of the present study, in which we have only considered one AV.

In order to characterize the efficiency of the cutters and following previous authors,[25] we focus on two synthetic quantities, flow rate and average fluid acceleration.

It is well known that the aspiration pressure affects the flow rate. In the present work, we found, for a given cutting frequency, this dependency was approximately linear. This is true for all cutters and both for BSS and AV (Figs. 4b, 7).

In order to compare directly SB and TDC devices, we reported the flow rate as a function of the cutting frequency for all vitreous cutters, keeping the driving pressure constant. We found, for a given cutter size and pressure, the 23- and 25-G TDC cutters are able to pump a flow significantly larger (almost doubled) than in the corresponding SB and, in all cases, the flow rate has a very weak dependency on the cutting frequency in the range of counts per minute investigated (Figs. 4a, Fig. 7a). This is essentially due to the fact that the needle port is never entirely closed during the cutting cycle.[14] Abulon et al.[14] performed experiments using 23- and 25-G dual-pneumatic probes at 5000 and 7500 cpm with a different vitrectomy system operated at various vacuum settings. The flow rates reported by the authors are significantly smaller compared with those measured in the present study using the TDC probes of the corresponding size, regardless of the cut rate.

The flow rate is significantly reduced in the case of AV with respect to BSS. For example, in the case of the 23-G TDC cutter, the flow rate is reduced from approximately 28 to 13 mL/min at a pressure of 600 mm Hg and cutting frequency of 6000 cpm. Similar results were observed for all cutters, even if this reduction is less dramatic as the cutter dimension decreased. It is difficult to compare the present results obtained with AV regarding the flow rates with published data because, in all previous studies, measurements were taken on different media without reporting their rheologic properties.

With regard to fluid acceleration, the averaged accelerations measured in BSS and AV showed similar dependency on the pressure and cutting frequency (Figs. 4, 7). The values of acceleration measured in the case of AV were lower compared with the same experimental conditions with BSS as a consequence of the fact that the flow rate is smaller in the former case.

The experiments performed in shaving mode were all characterized by a similar flow rate and similar acceleration (Fig. 8).

Rossi et al.[25] proposed a scattergram plot reporting BSS and egg albumen average acceleration versus flow rate in order to classify cutter behavior in terms of efficiency and safety. In principle, the most suitable blade/settings combination would be characterized by high flow and low acceleration. We propose a similar plot in Figure 8, containing data obtained with both BSS and AV. For BSS we used the clinical parameters reported in the Table. For the AV we did not explicitly reproduce the clinical parameters; however, owing to the weak dependency of the flow rate on the cutting frequency (see Fig. 7a), we used the data taken at slightly different cutting frequencies to produce the plot. The 27-G TDC reaches flow rate values comparable with the larger size 23- and 25-G SB cutters, both in BSS and AV. Although the flow rates were comparable, the resulting acceleration is much smaller for the 27-G TDC than for the 23- and 25-G SB. TDC cutters, regardless their dimensions, produce higher flow rates with accelerations comparable to their SB counterparts.

The reader is probably now tempted to directly compare the results Figure 8 with the corresponding the results reported in Rossi et al.[25] We first note that we computed the acceleration according to Equation 1, while Rossi et al.[25] only considered the first term of the equation. However, being the convective term more than two orders of magnitude smaller than the local time derivative of the velocity, the different approach adopted by Rossi et al.[25] seems to be justified. Moreover, as mentioned above, the value of the spatially averaged acceleration strongly depends on the averaging area, because the flow intensity rapidly decays with distance from the cutter port. Rossi et al.[25] did not explicitly declare the averaging area. The values obtained in the present work are invariably smaller than those reported in Rossi et al.[25] Assuming that the authors used the entire field of view shown in their images, which is significantly larger than the circle of 3 mm of radius used here, this would imply that we calculated significantly smaller accelerations than they did. Obviously, the differences in the device itself may contribute to this mismatch in the results.

In conclusion, we found that for all cutters the flow rate depends linearly on the aspiration pressure and it is almost double with TDC probes. Moreover, the flow rate is almost independent of the cutting frequency both for SB and TDC cutters in the range of frequencies investigated. The magnitude of fluid acceleration depends on the cut rate and on the aspiration pressure, without a significant increase with TDC with respect to SB cutter probes at constant flow rate. Comparing TDC and SB vitrectomy probes the increase of flow rate with TDC is much more pronounced than the corresponding increase of acceleration, therefore, we can state that the former has more efficient fluidics than the latter. The behavior of the cutters strongly depends on the rheology of the vitreous and this aspect deserves further specific investigations.

Acknowledgments

Supported by grants from by DORC International, Zuidland, The Netherlands through a research grant to the Department of Civil, Chemical, and Environmental Engineering. DORC that also provided the EVA system for the experimental measurements.

Disclosure: **M.R. Romano**, None; **A. Stocchino**, None; **M. Ferrara**, None; **A. Lagazzo**, None; **R. Repetto**, None

References

1. Oliveira PRC, Berger AR, Chow DR. Vitreoretinal instruments: vitrectomy cutters, endoillumination and wide-angle viewing systems. *Int J Retina Vitreous*. 2016;2:28.
2. Rossi T, Querzoli G, Angelini G. Fluid dynamics of vitrectomy probes. *Retina*. 2014;34:558–567.
3. Pavlidis M. Two-dimensional cutting (TDC) vitrectome: in vitro flow assessment and prospective clinical study evaluating core vitrectomy efficiency versus standard vitrectome. *J Ophthalmol*. 2016;2016:3849316.
4. Rossi T, Querzoli G, Malvasi C, Iossa M, Angelini G, Ripandelli G. A new vitreous cutter blade engineered for constant flow vitrectomy. *Retina*. 2014;34:1487–1491.
5. Abulon DJK, Buboltz DC. Porcine vitreous flow behavior during high-speed vitrectomy up to 7500 cuts per minute. *Transl Vis Sci Technol* 2016;5(1):7.
6. Stalmans P. Enhancing visual acuity. In: Oh H, Oshima Y. *Microincision Vitrectomy Surgery*. Basel: Karger Publishers; 2014:23–30.
7. Steel DHW, Charles S. Vitrectomy fluidics. *Ophthalmologica*. 2011;226:27–35.

8. Rossi T, Querzoli G, Angelini G, et al. Hydraulic resistance of vitreous cutters: the impact of blade design and cut rate. *Transl Vis Sci Technol*. 2016; 5(4);1.
9. Teixeira A, Chong L, Matsuoka N, et al. An experimental protocol of the model to quantify traction applied to the retina by vitreous cutters. *Invest Ophthalmol Vis Sci*. 2010;51:4181–4186.
10. Teixeira A, Chong L, Matsuoka N, et al. Novel method to quantify traction in a vitrectomy procedure. *Br J Ophthalmol*. 2010;94:1226–1229.
11. Teixeira A, Chong LP, Matsuoka N, et al. Vitreoretinal traction created by conventional cutters during vitrectomy. *Ophthalmology*. 2010; 117;1387–1392.
12. Thompson JT. Advantages and limitations of small gauge vitrectomy. *Surv Ophthalmol*. 2011; 56;162–172.
13. Magalhaes O Jr, Chong L, DeBOER C, et al. Vitreous dynamics: vitreous flow analysis in 20-, 23-, and 25-gauge cutters. *Retina*. 2008;28:236–241.
14. Abulon DJK, Buboltz DC. Performance comparison of high-speed dual-pneumatic vitrectomy cutters during simulated vitrectomy with balanced salt solution. *Tranls Vis Sci Technol*. 2015; 4(1):6.
15. Diniz B, Fernandes RB, Ribeiro RM, et al. Analysis of a 23-gauge ultra high-speed cutter with duty cycle control. *Retina*. 2013;33:933.
16. Fernandes RAB, Diniz B, Falabella P, et al. Fluidics comparison between dual pneumatic and spring return high-speed vitrectomy systems. *Ophthalmic Surg Lasers Imaging Retina*. 2015; 46:68–72.
17. Zehetner C, Moelgg M, Bechrakis E, Linhart C, Bechrakis NE. In vitro flow analysis of novel double-cutting open-port, ultrahigh-speed vitrectomy systems [published online ahead of print October 9, 2017]. *Retina*. doi: 10.1097/IAE.0000000000001882.
18. Abulon DJK. Vitreous flow rates through dual pneumatic cutters: effects of duty cycle and cut rate. *Clin Ophthalmol*. 2015;9:253.
19. Adrian RJ. Twenty years of particle image velocimetry. *Exp Fluids*. 2005;39:159–169.
20. Kummer MP, Abbott JJ, Dinser S, Nelson BJ. Artificial vitreous humor for in vitro experiments. *Conf Proc IEEE Eng Med Biol Sci*. 2007;2007: 6407–6410.
21. Tanner RI. Engineering Rheology, 2 ed. City, State/country: Oxford University Press; 2000.
22. Nickerson CS, Park J, Kornfield JA, Karageozian H. Rheological properties of the vitreous and the role of hyaluronic acid. *J Biomech*. 2008;41: 1840–1846.
23. Swindle KE, Hamilton PD, Ravi N. In situ formation of hydrogels as vitreous substitutes: viscoelastic comparison to porcine vitreous. *J Biomed Mat Res A*. 2008;87:656–665.
24. Sharif-Kashani P, Hubschman JP, Sassoon D, Kavehpourlee HP. Rheology of the vitreous gel: effects of macromolecule organization on the viscoelastic properties. *J Biomech*. 2011;44:419–423.
25. Rossi T, Querzoli G, Angelini G, et al. Introducing new vitreous cutter blade shapes: a fluid dynamics study. *Retina*. 2014;34:1896–1904.
26. Meskauskas J, Repetto R, Siggers JH. Oscillatory motion of a viscoelastic fluid within a spherical cavity. *J Fluid Mech*. 2011;685:1–22.
27. Bonfiglio A, Lagazzo A, Repetto R, Stocchino A. An experimental model of vitreous motion induced by eye rotations. *Eye Vis*. 2015;2:10.